Int. J. Heat Mass Transfer. Vol. 35, No. 8, pp. 1881–1892, 1992
Printed in Great Britain

0017–9310/92 $5.00+0.00

Prandtl number effects on laminar mixed convection heat transfer in a lid-driven cavity

M. K. MOALLEMI and K. S. JANG
Department of Mechanical and Industrial Engineering, Polytechnic University,
333 Jay Street, Brooklyn, NY 11201, U.S.A.

(*Received* 7 *March* 1991 *and in final form* 14 *August* 1991)

Abstract—This paper considers the flow and heat transfer in a square cavity where the flow is induced by a shear force resulting from the motion of the upper lid combined with buoyancy force due to bottom heating. The work is motivated by the application in the production of plane glass where the glass sheet is pulled over a bath of molten metal while being cooled and solidified. The numerical simulations, therefore, are performed for two-dimensional laminar flow ($100 \leqslant Re \leqslant 2200$), and effects of small to moderate Prandtl numbers (i.e. $0.01 < Pr < 50$) on the flow and the heat transfer in the cavity are investigated for different values of Richardson number. The temperature and the flow fields in the cavity are calculated and presented to illustrate the strong influence of Prandtl number. The local and average Nusselt numbers are also reported for different values of *Re*, *Ri*, and *Pr*.

1. INTRODUCTION

MIXED-CONVECTION flow and heat transfer occur frequently in engineering and natural situations. One important configuration is a lid-driven (or shear-driven) flow in a differentially heated/cooled cavity, which has applications in crystal growth, flow and heat transfer in solar ponds [1], dynamics of lakes [2], and thermal-hydraulics of nuclear reactors [3]. Flow in cavities driven by a combined shear and buoyancy force also arises in industrial processes such as food processing, and float glass production [4].

The lid-driven cavity flow has served over and over again as a standard test case for the evaluation of numerical solution procedures for the Navier–Stokes equations [5–10]. In these works, however, the effects of buoyancy were not addressed since isothermal cavity flows were studied [5–8], or the boundary conditions represented thermally stable (i.e. stratified) situations [9–10]. Flow in thermally stratified and isothermal lid-driven cavities has been the subject of extensive investigations at the Environmental Fluid Mechanics Laboratory at Stanford University (e.g. Koseff *et al.* [11], Koseff and Street [12, 13] and Freitas and Street [14]). Through flow visualization, velocity measurements, and numerical simulations, recirculation flow patterns were characterized over a wide range of *Re* and *Gr*. These revealed that three-dimensional features, such as corner eddies near the end walls, and Taylor–Gortler-like longitudinal vortices, have significant influences on the flow for Reynolds numbers as low as 3200. These works emphasized the fluid mechanics aspects of the problem and did not deal with the heat transfer issues vigorously [11, 12].

Torrance *et al.* [15] numerically investigated both thermally stable and unstable shear-driven flows ($-10^6 < Gr < +10^6$) in cavities with depthwise aspect ratios of 0.5, 1 and 2. These simulations were performed for fixed values of $Re = 100$ and $Pr = 1$, with the three cavity walls at a constant temperature different from the temperature of the top driving lid. Their results indicated that the Richardson number ($Ri \equiv Gr/Re^2$) was a governing parameter of the problem. They particularly concluded that the flow pattern in the cavity was influenced by the buoyancy if the absolute value of *Ri* was greater than unity. However, the effects of buoyancy on the heat transfer rate in the cavity were not characterized quantitatively.

Mixed convection heat transfer in a lid-driven cavity was recently investigated by Prasad and Koseff [16]. In a series of experiments which were performed on a cavity filled with water, the heat flux was measured at different locations over the hot cavity floor for a range of *Re* and *Gr*. Their results indicated that the overall (i.e. area-averaged) heat transfer rate was a very weak function of *Gr* for the range of *Re* examined ($2200 \leqslant Re \leqslant 12\,000$). The data were correlated by Nusselt number vs Reynolds number, as well as Stanton number vs Reynolds number relations. The point that heat transfer is independent of buoyancy is rather surprising considering the range of *Gr* examined, i.e. $10^7 \leqslant Gr \leqslant 5 \times 10^9$. It is among the objectives of this work to provide an explanation for this point.

In some mixed convection literature [15–17] Richardson number has been reported to be the indicator of the relative importance of buoyancy induced flow. This observation is based on analyses and experiments on fluids with Prandtl numbers of order of unity, and cannot be treated as a universal rule. In fact, through a scale analysis of mixed convection flow over a vertical wall, Bejan [18] showed that the criterion for the transition from forced convection dominant flow to natural convection dominant flow was not the same for $Pr > 1$ and $Pr < 1$ fluids. The transition criterion

NOMENCLATURE

A	aspect ratio, and constant for equation (12)
B	constant for equation (12)
g	gravitational acceleration [m s^{-2}]
Gr	Grashof number, $g\beta(T_H - T_C)L^3/\nu^2$
h	heat transfer coefficient [W m^{-2} K^{-1}]
k	thermal conductivity [W m^{-1} K^{-1}]
L	cavity depth and width [m]
Nu	Nusselt number, dimensionless heat transfer coefficient, $-\partial\Theta/\partial Y = hL/k$
p	pressure [N m^{-2}]
P	dimensionless pressure, $p/\rho U_L^2$
Pr	Prandtl number, ν/α
Re	Reynolds number, $U_L L/\nu$
Ri	Richardson number, Gr/Re^2
T	temperature [K]
(u, v)	horizontal and vertical velocity components [m s^{-1}]
(U, V)	dimensionless velocity components, $(u, v)/U_L$
U_L	lid velocity [m s^{-1}]
(x, y)	horizontal and vertical coordinates [m]
(X, Y)	dimensionless coordinates, $(x, y)/L$.

Greek symbols

α	thermal diffusivity [m^2 s^{-1}]
β	coefficient of thermal expansion [K^{-1}]
Θ	dimensionless temperature, $(T - T_C)/(T_H - T_C)$
ν	kinematic viscosity [m^2 s^{-1}].

Subscripts

C	cold
F	forced convection
H	hot
L	lid
N	natural convection.

is not yet validated for $Pr \ll 1$ fluids, due to the non-existence of experimental data for this range of Pr. Recently, however, Mohamad and Viskanta [19] reported on the effects of Pr on the onset of instability in a shallow lid-driven cavity heated from below. Through a linear stability analysis, they found that Pr influenced the conditions for the initiation of the mixed convection regime.

This paper considers the flow and heat transfer in a square cavity where flow is induced by a shear force resulting from the motion of the upper lid combined with the buoyancy force due to bottom heating. The work is motivated by the application in the production of plane glass where a glass sheet is pulled over a bath of molten metal while being cooled to solidify. The numerical simulations, therefore, are performed for two-dimensional laminar flows. The effects of small to moderate Prandtl numbers (i.e. $0.01 < Pr < 50$) on the flow and heat transfer in the cavity are investigated for different values of Reynolds and Richardson numbers. The temperature and flow fields in the cavity are presented to illustrate the strong influence of Prandtl number. The effects of Pr on the variation of the heat transfer distribution over the cavity floor, and the driving lid are discussed, and correlations for the average Nusselt number are reported.

2. PROBLEM FORMULATION

Fluid flow and heat transfer are modeled in a two-dimensional square cavity of width L in which the top (lid) surface moves across the cavity from left to right at a constant speed U_L, as shown in Fig. 1. The two vertical walls of the cavity are insulated, and the lid and bottom surfaces are maintained at constant temperatures, T_C and T_H, respectively, with $T_C < T_H$. The flow is assumed to be laminar, and the fluid properties are constant except for the density in the buoyancy term (the Boussinesq approximation).

The governing equations of the problem are expressions of conservation of mass, momentum, and thermal energy. Using L, U_L, and $(T_H - T_C)$ as length, velocity, and temperature scales, the governing equations are non-dimensionalized to yield

$$\frac{\partial U}{\partial X} + \frac{\partial V}{\partial Y} = 0 \tag{1}$$

$$U\frac{\partial U}{\partial X} + V\frac{\partial U}{\partial Y} = -\frac{\partial P}{\partial X} + \frac{1}{Re}\left(\frac{\partial^2 U}{\partial X^2} + \frac{\partial^2 U}{\partial Y^2}\right) \tag{2}$$

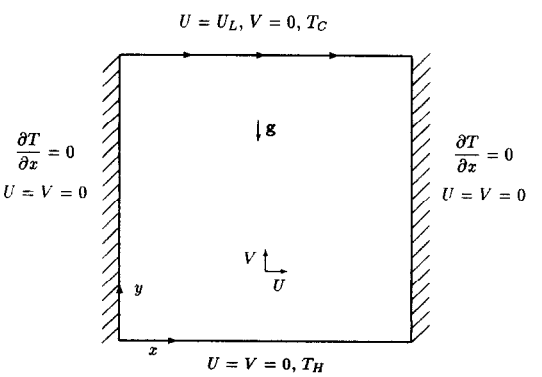

FIG. 1. Schematic diagram of the cavity and boundary conditions.

$$U\frac{\partial V}{\partial X}+V\frac{\partial V}{\partial Y}=-\frac{\partial P}{\partial Y}+\frac{1}{Re}\left(\frac{\partial^2 V}{\partial X^2}+\frac{\partial^2 V}{\partial Y^2}\right)+\frac{Gr}{Re^2}\Theta \quad (3)$$

$$U\frac{\partial \Theta}{\partial X}+V\frac{\partial \Theta}{\partial Y}=\frac{1}{Re\,Pr}\left(\frac{\partial^2 \Theta}{\partial X^2}+\frac{\partial^2 \Theta}{\partial Y^2}\right). \quad (4)$$

The governing parameters of the problem are Reynolds, Grashof, and Prandtl numbers which are defined in the Nomenclature. The coupling between the heat transfer and the fluid flow in the cavity is through the buoyancy term in the y-momentum equation, equation (3), which has $Gr/Re^2 \equiv Ri$ as a dimensionless coefficient.

The velocity and temperature boundary conditions are shown in Fig. 1 and have the following dimensionless forms:

$$\begin{aligned}
&\text{at } X=0 \text{ and } X=1 \quad U=V=0 \quad \text{and} \quad \frac{\partial \Theta}{\partial X}=0\\
&\text{at } Y=0 \quad U=0, \quad V=0 \quad \text{and} \quad \Theta=1\\
&\text{at } Y=1 \quad U=1, \quad V=0 \quad \text{and} \quad \Theta=0.
\end{aligned} \quad (5)$$

3. METHOD OF SOLUTION

The dimensionless governing equations are discretized using the control volume approach with the power-law scheme [20] for the calculations of the fluxes at the faces of the control volumes. The SIMPLER algorithm [20] is used with the inertia relaxation method of ref. [3] to accelerate convergence. To resolve the large velocity and temperature gradients in the boundary layers near the cavity walls, a nonuniform grid system was used in both X- and Y-directions. The position of the control surfaces of the grid system were determined with an exponentially clustering scheme. A series of grid sensitivity runs were performed on nonuniform grids ranging from 22×22 to 52×52, which suggested that grid independent results could be achieved using a 42×42 grid. The results of two nonuniform grids of 42×42 and 52×52 for $Re=1000$, $Gr=10^6$, and $Pr=0.1$ revealed differences less than 1% in the streamlines and isotherms. The solution procedure is iterative and requires initial guesses for all the dependent variables. To facilitate the convergence of the solution for a given set of parameters, the converged solution of a case with smaller Ri or Re was used as the initial guess. Sensitivity tests have indicated that the final results were independent of the initial guess.

For any set of input parameters, the solution was considered converged if

$$\frac{|\psi^{k+1}(i,j)-\psi^{k}(i,j)|}{\text{Max}\,|\psi^{k+1}(i,j)|}<10^{-3} \quad \text{and} \quad \left|1.0-\frac{\overline{Nu_C}}{\overline{Nu_H}}\right|<10^{-3} \quad (6)$$

where i and j refer to the computational nodes, k is the iteration loop counter, ψ is u, v, or T, and $\overline{Nu_H}$ and $\overline{Nu_C}$ are area-averaged Nusselt numbers on the lid and bottom surfaces, respectively. When the above criteria were satisfied, the residual source of mass was less than 10^{-7} for all the cases examined. The convergence of the local heat transfer rate over the bottom surface, as judged by the position and magnitude of its relative maximum, was within 0.5% when the criteria of equation (6) were satisfied. Depending on the input parameters, 1000 to 1800 iterations were required for the solution to converge, with cases with lower Ri or higher Pr requiring a fewer number of iterations.

The numerical procedure was validated by performing simulations of isothermal flow in a square cavity with a driving lid for $Re=400$ and 1000. The results of these simulations were compared with the calculations of Schreiber and Keller [7], and Thompson and Ferziger [8]. These comparisons revealed better than 95% agreement in the strength and position of the primary [7, 8] and secondary [7] eddies. The solution procedure was also validated by comparing the predicted heat transfer rates with the experimental results of Prasad and Koseff [16]. The predicted area-averaged heat transfer rates agreed to within 5% of the experimental data for $Pr=6.0$, $Re=2200$, and $Gr=10^7$ and 4×10^7.

4. RESULTS AND DISCUSSIONS

The main objective of this investigation was to study the effects of Pr on the flow and heat transfer in a square cavity driven by a combined shear and buoyancy force. Forty-six numerical simulations were performed for a range of Pr, i.e. $Pr=0.01$, 0.1, 6.0, 7.1, and 50. With four values for Re (i.e. $Re=100$, 500, 1000, and 2200), and four values of Gr (i.e. $Gr=10^4$, 10^5, 10^6, and 10^7), these simulations covered a range of Ri from 0.01 to 10.

The predicted flow and temperature fields for $Re=1000$, and $Gr=10^4$ (i.e. constant value of $Ri=0.01$), and for three different values of Pr are shown in Fig. 2. The flow fields for all the three cases are essentially established by the shear induced by the moving lid. This may be examined by recalling the general features of the lid-driven cavity flow in the absence of buoyancy. The fluid flow in a two-dimensional lid-driven cavity is characterized by (a) a primary recirculating eddy of the size of the cavity generated by the lid dragging the adjacent fluid; (b) a secondary eddy formed in the apex of the vertical wall and the bottom surface (referred to as the downstream secondary eddy, DSE) as a result of frictional losses and stagnation pressure; (c) another secondary eddy (referred to as the upstream secondary eddy, USE) formed in the upstream lower corner due to the negative pressure gradient generated by the primary circulating fluid as it deflects upward over the upstream vertical wall; and (d) a third secondary eddy which

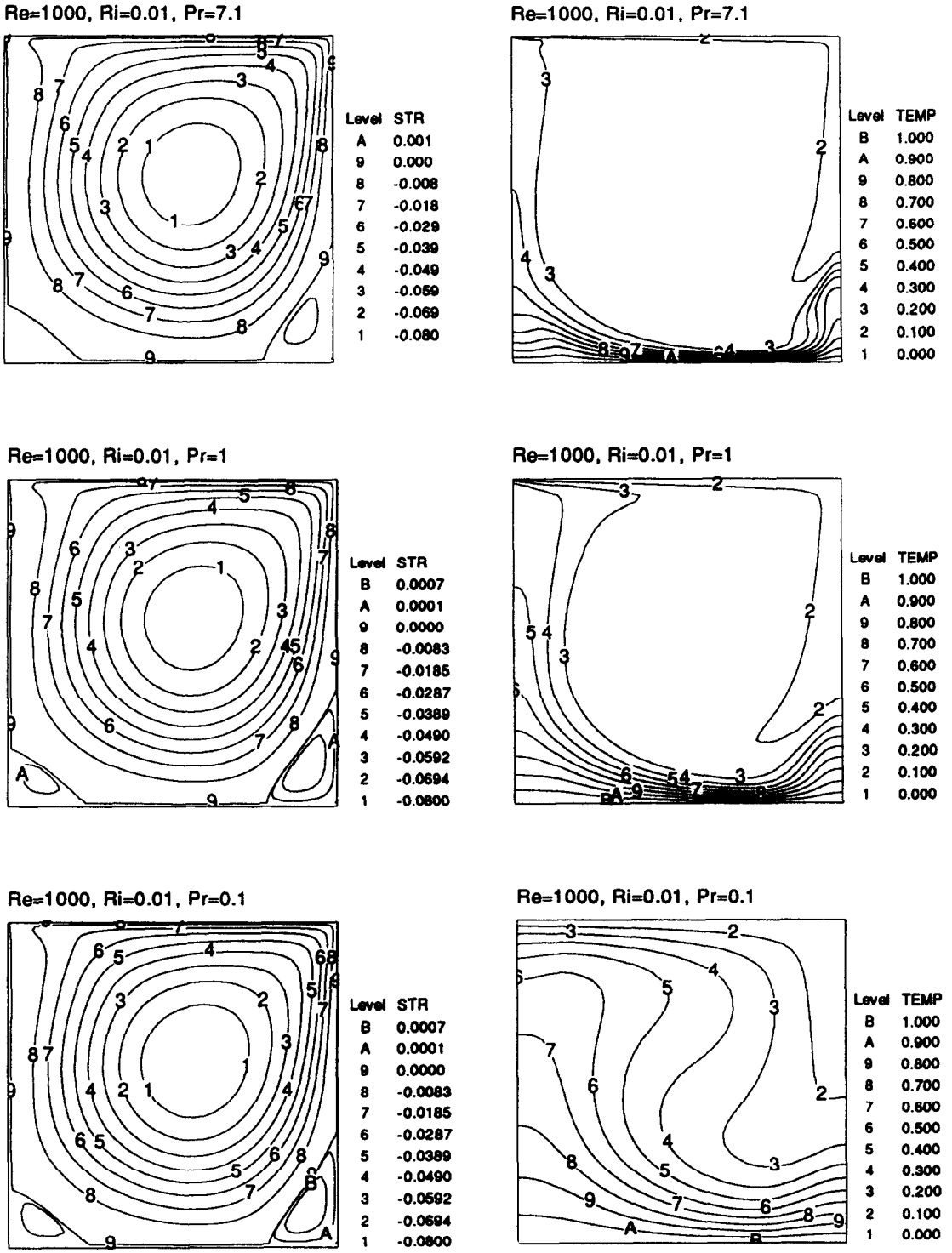

FIG. 2. Effect of Pr on the flow temperature fields in the cavity, for $Re = 1000$ and $Gr = 10^4$.

may develop on the vertical wall near the lid, for $Re \geqslant 1000$, as the lid draws fluid from the corner into the lid boundary layer [11–13]. All these features are present in the flow fields shown in Fig. 2, regardless of the value of Pr. Moreover, the size, position, and strength of the secondary eddies are almost identical for the three cases presented in this figure. These confirm the established notion that for $Ri \ll 1$, the flow

in the cavity is defined by the shear action of the moving lid [15], and thus, is independent of Pr which defines the temperature and buoyancy variations in the cavity.

The temperature distributions in the cavity, shown on the right side of Fig. 2, exhibit strong dependence on Pr. These indicate that the thermal boundary layers over the bottom and the lid surfaces thicken as Pr is reduced. The large isothermal region which extends over most of the cavity for $Pr = 7.1$, shrinks with decreasing Pr, and disappears for $Pr \leqslant 0.1$. The strong dependence of the temperature distribution on Pr does not reflect on the flow pattern in the cavity which again demonstrates the insignificant contribution of buoyancy in the flow development for $Ri \ll 1$.

Figure 3 presents the flow and temperature fields calculated for $Re = 500$, $Gr = 10^5$ (i.e. constant value of $Ri = 0.4$), and for $Pr = 7.1$, 1.0, and 0.1. The flow fields of this figure indicate to a more significant contribution of buoyancy in defining the flow pattern in the cavity, as compared with the flow fields of Fig. 2. The upstream secondary eddies have vanished, and the downstream secondary eddies have changed size. On the upstream wall, buoyancy assists the core flow to make a sharp turn, and thus, the secondary eddy at the upstream corner disappears. On the downstream wall, however, buoyancy is opposing the core flow and causes the downcoming boundary layer to detach from the wall at a larger Y, resulting in a larger eddy. The effects of Pr on the temperature distribution in the cavity in this figure are similar to those of Fig. 2, i.e. large isothermal core region for large Pr, and very thick thermal boundary layers for small Pr. For the cases of Fig. 3, however, a change in Pr results in a change in the flow pattern in the cavity, confirming the important role of buoyancy in defining the flow field in the cavity. For large values of Pr, since the core is isothermal, the influence of buoyancy is limited to the boundary layers, and appears in the form of reduction in the size or position of the secondary eddies. For small values of Pr, the effects of buoyancy manifest in the boundary layers, and also in the core of the cavity. Therefore, a reduction in Pr will result in a stronger primary eddy while affecting the sizes and positions of the secondary eddies, as well.

The flow and temperature fields in the cavity for $Re = 1000$ and $Gr = 10^6$ are presented in Fig. 4. This figure shows that for $Ri = 1.0$ the fluid flow in the cavity is established by a relatively balanced interaction of the two driving mechanisms involved, with a strong dependence on Pr. For Pr equal to unity, the balance of the shear and buoyancy effects is manifested in the formation of two eddies of almost equal size. The upper eddy is driven by the moving lid, and encapsulates an isothermal core. This is in fact the primary eddy which is deformed due to the opposing action of the buoyancy. The eddy in the lower half of the cavity is driven by buoyancy, and is the enlarged form of the DSE. For Pr greater than unity, the heat transfer is mostly via convection in the boundary layers, the core of the cavity is isothermal, and the buoyancy effects are only significant near the cavity wall. And these together result in the enlargement of the DSE, and the elimination of the USE. For $Pr \ll 1.0$, the heat transfer in the cavity is mostly due to conduction, resulting in a rather gradual variation of temperature in the cavity, and therefore, a small buoyancy field. In the bottom flow field in Fig. 4, the presence of USE and upper secondary eddies in the cavity is the result of weak buoyancy or, in other words, strong shear-induced recirculation.

The flow and temperature fields for $Ri = 4$ ($Re = 500$ and $Gr = 10^6$) illustrate similar effects and interactions, as shown in Fig. 5. Comparing the flow fields in Figs. 4 and 5 shows the influence of a change in shear at constant Gr for different values of Pr. In the top rows ($Pr = 7.1$), a decrease in Re results in significant change in the flow structure, i.e. the enlargement of the DSE. Whereas, for $Pr = 0.1$, a decrease in Re causes a change in the strength of the primary eddy, with little effect on the secondary eddies or the temperature field. The influence of a change in buoyancy on flow and heat transfer in the cavity at constant lid shear may be revealed in a comparison of Figs. 3 and 5. For large values of the Prandtl number, i.e. $Pr \geqslant 1.0$, an increase in Gr results in significant change in the secondary eddies, as well as the primary eddy. This is due to the fact that for this range of Pr, the flow in the cavity is boundary layer type. For $Pr < 1.0$, however, the cavity flow is more of a core flow type, and an increase in buoyancy results in a stronger primary eddy and this manifests in the formation of an upper secondary eddy on the vertical wall near the lid, and the resurgence of the USE.

The variations of local Nusselt number over the lid and bottom surfaces for different values of Re, Gr, and Pr are presented in Figs. 6–10. Over the cold lid surface, the heat transfer rate generally drops in the direction of the lid motion due to the formation and growth of the boundary layer over this surface. Over the bottom hot surface, however, the variation of the local heat transfer rates is more complex, and exhibits local maxima and minima which are defined by the action of the primary and secondary eddies on this surface. The local Nu_H has a relative maximum at a point that cold fluid impinges on the cavity floor. The drop in the heat transfer subsequent to an impingement point is due to the formation and growth of boundary layers over the cavity floor. The points of relative minimum Nu_H correspond to the points of detachment of these boundary layers from the cavity floor. These may be examined by referring to the corresponding flow fields presented in Figs. 2–5.

In Figs. 6 and 7, for which $Ri < 1$, the local and area-averaged heat transfer rates over the lid as well as the floor surfaces increase with an increase in Pr. This trend is consistent over both surfaces since neither the dashed lines nor the solid lines cross each other. For these cases, it may be concluded that the heat transfer

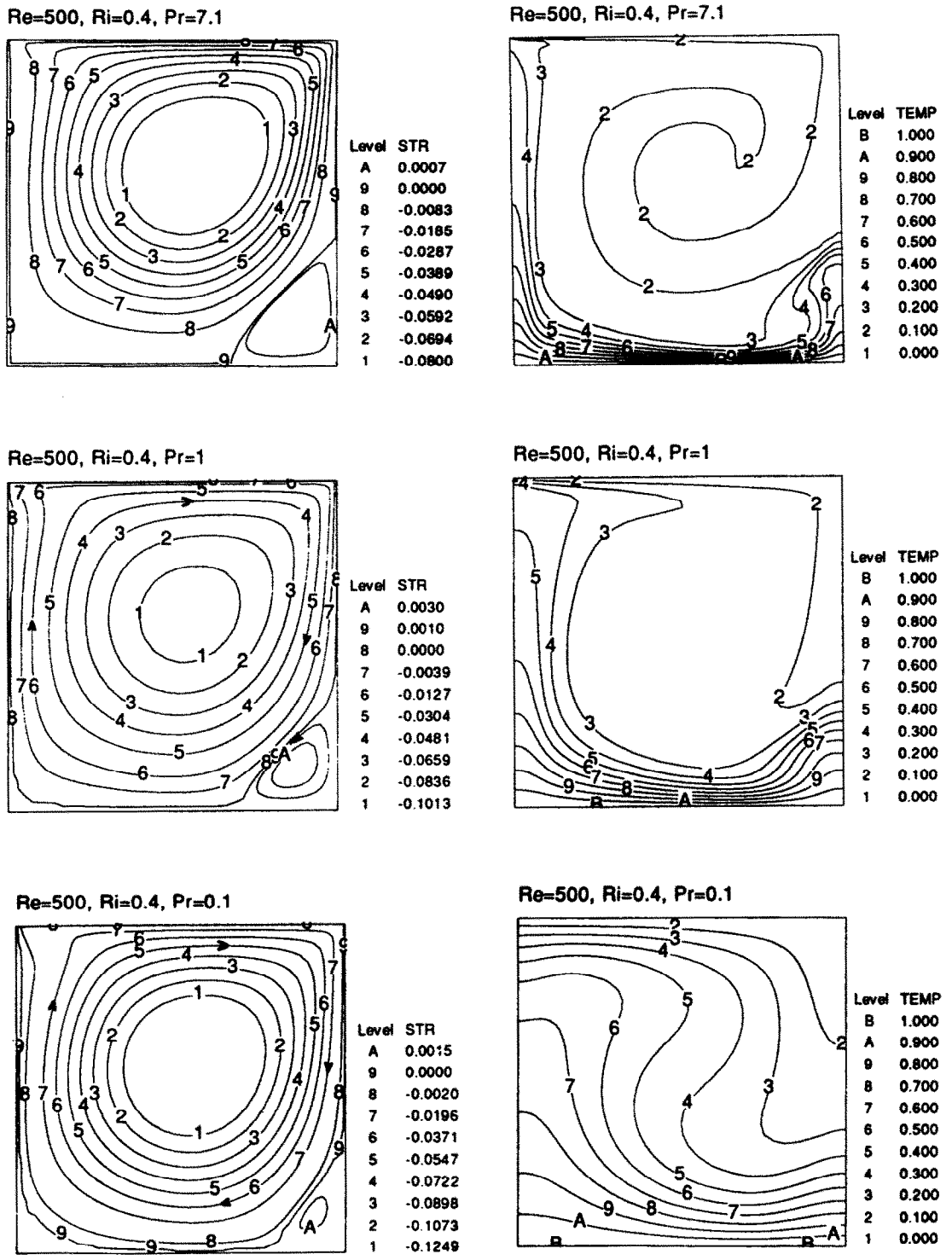

FIG. 3. Effect of Pr on the flow and temperature fields in the cavity, for $Re = 500$ and $Gr = 10^5$.

in the cavity is defined by the shear flow that dictates the primary recirculation in the cavity, since the form of variation of Nu_C along the lid does not change with Pr. The effect of buoyancy on the local heat transfer rate from the cavity floor is recognized to be minimal, as the positions of maximum and minimum heat transfer rates do not noticeably change with a change in Pr. The small change in the local variation of Nu_H with Pr is due to the weak influence of buoyancy on the secondary eddies.

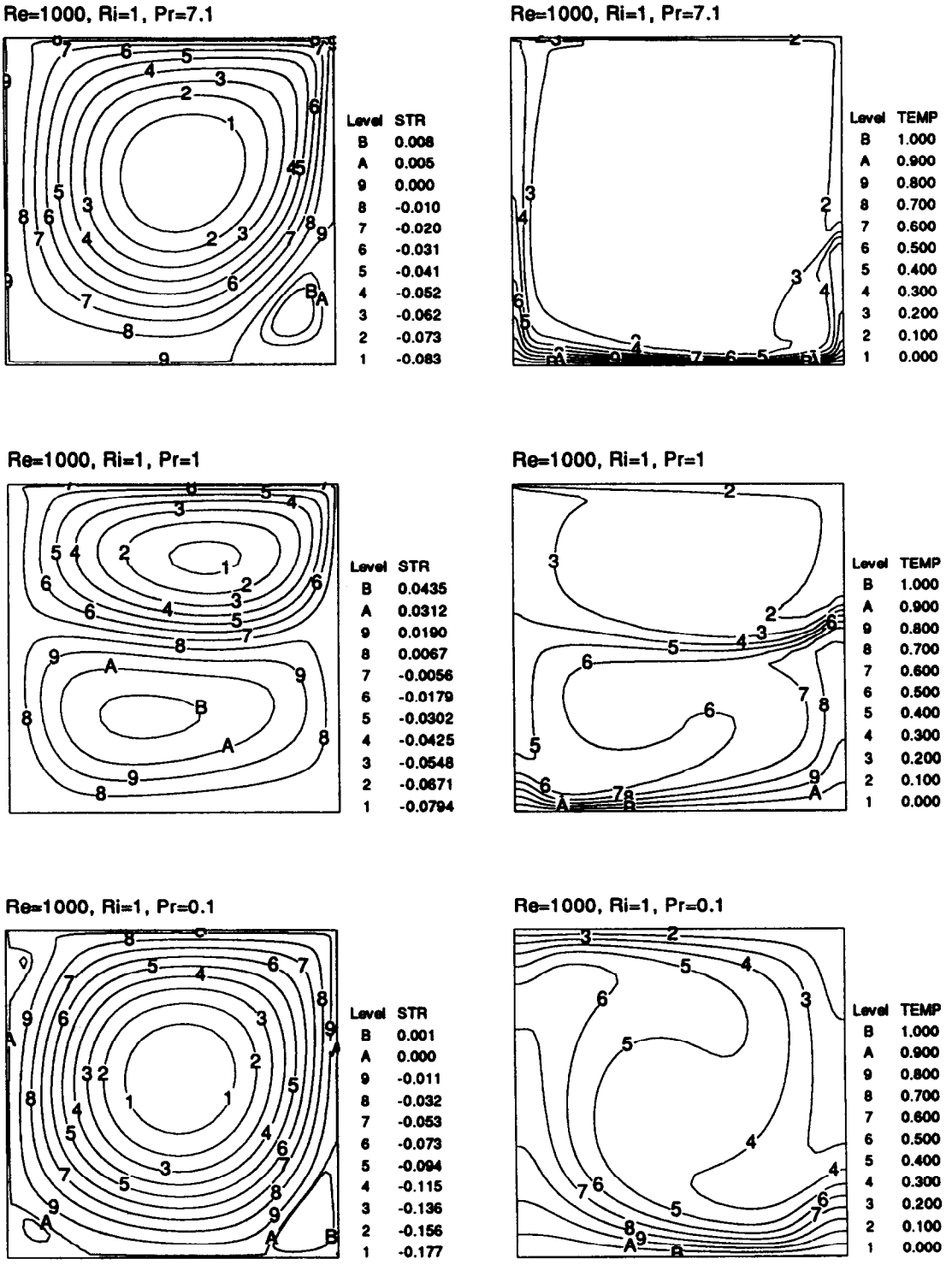

FIG. 4. Effect of Pr on the flow and temperature fields in the cavity, for $Re = 1000$ and $Gr = 10^6$.

In Figs. 8 and 9 ($Ri \geqslant 1$), the variations of Nu_H and Nu_C illustrate stronger dependence on Pr, indicating a more significant contribution of buoyancy to heat transfer and fluid flow in the cavity. For Nu_H variations, the points of maxima and minima again correspond to the points of cold flow impingement on the floor, and points of boundary layer detachment from the floor, respectively. In these figures, the effects of Pr on Nu_H and Nu_C may be noted to be both quantitative (i.e. mostly higher heat transfer rates for

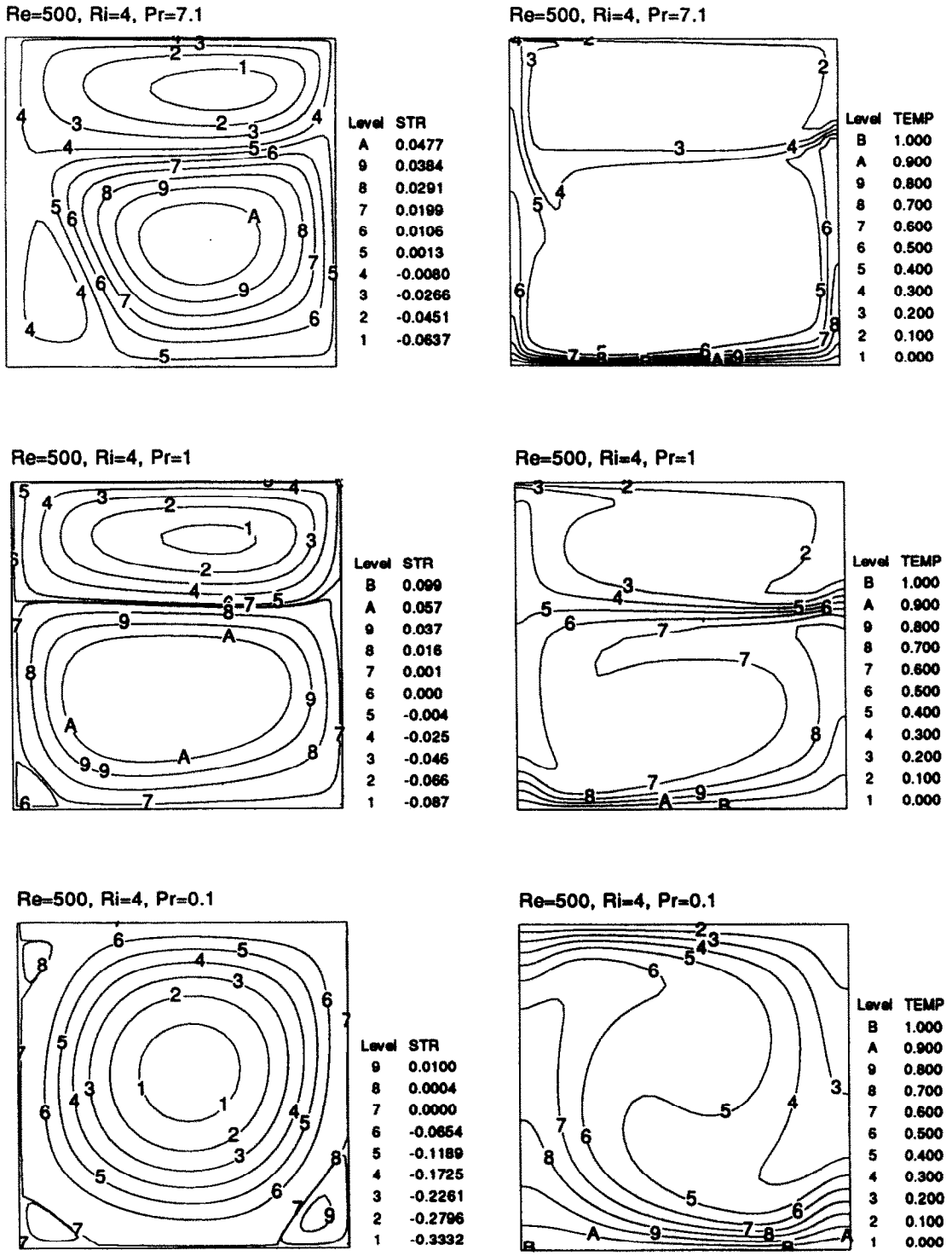

FIG. 5. Effect of Pr on the flow and temperature fields in the cavity, for $Re = 500$ and $Gr = 10^6$.

larger values of Pr) and qualitative (i.e. changes in the positions of maximum and minimum Nu_H with a change in Pr). In either sense, however, the influence is more pronounced for larger Pr. This confirms the earlier observations that for $Ri \geqslant 1.0$ the buoyancy effects are felt by both the primary and the secondary eddies, particularly for cases with $Pr \geqslant 1.0$.

The influence of Pr on the variation of the area-averaged heat transfer rate with Ri, for different values of Re, is presented in Fig. 10. The experimental results

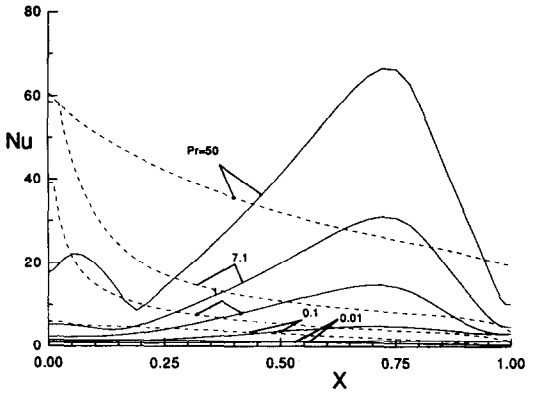

FIG. 6. Variations of the local Nu over the cavity floor (solid lines), and the lid (dash lines), for $Re = 1000$ and $Gr = 10^4$ ($Ri = 0.01$).

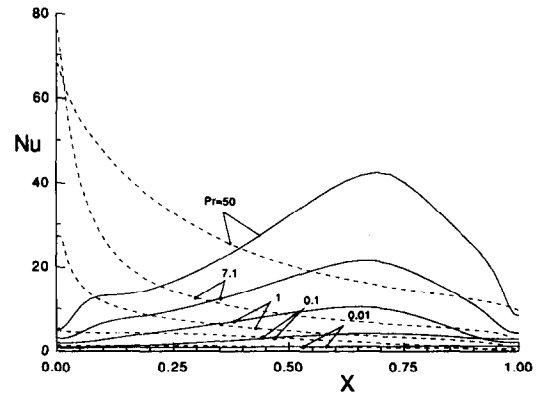

FIG. 7. Variations of the local Nu over the cavity floor (solid lines), and the lid (dash lines), $Re = 500$ and $Gr = 10^5$ ($Ri = 0.4$).

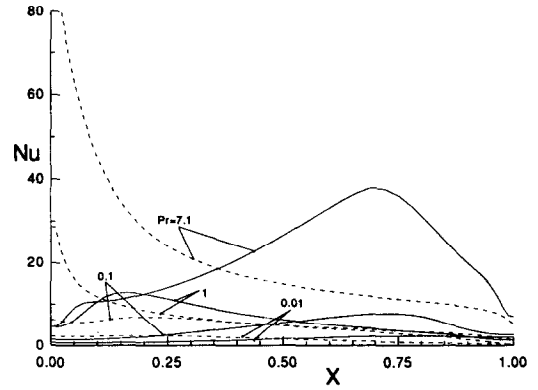

FIG. 8. Variations of the local Nu over the cavity floor (solid lines), and the lid (dash lines), $Re = 1000$ and $Gr = 10^6$ ($Ri = 1.0$).

of Prasad and Koseff [16], for water ($Pr = 6.0$) at $Re = 2200$ are also shown in the figure, which compare well with the results of simulations performed for the same set of parameters. The figure indicates a rapid drop of convective heat transfer in the cavity with a decrease in Pr. This drop which is also a function of Re brings the $\overline{Nu}$ to 1.03 for $Pr = 0.01$ and

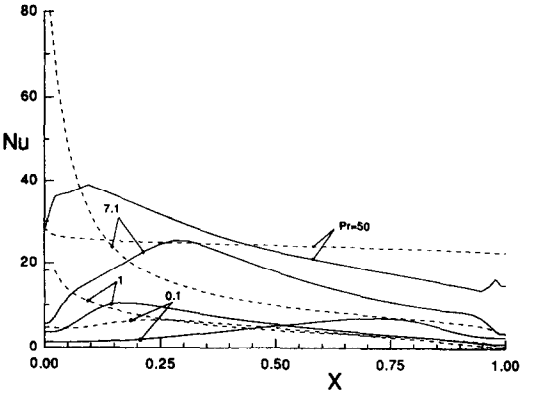

FIG. 9. Variations of the local Nu over the cavity floor (solid lines), and the lid (dash lines), $Re = 500$ and $Gr = 10^6$ ($Ri = 4.0$).

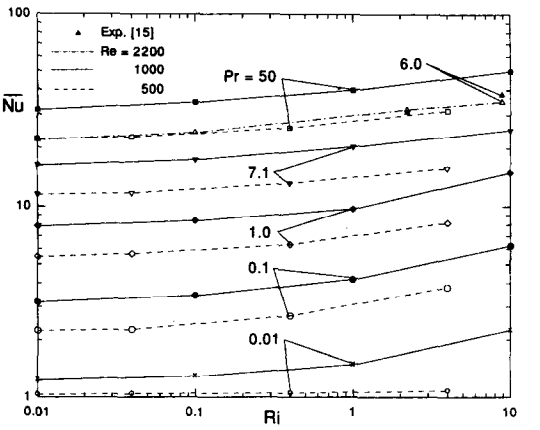

FIG. 10. Effect of Pr on the variation of averaged Nu with Ri.

$Re = 500$, only 3% above the conduction limit of unity. The results also illustrate that up to a minimum level of buoyancy, the heat transfer rate in the cavity is essentially via forced convection and independent of Ri. The departure from the forced convection heat transfer mechanism to a mixed convection one, for which $\overline{Nu} = f(Re, Ri)$, is noted to be a function of Pr.

Prasad and Koseff [16] have correlated their experimental results as

$$\overline{Nu} \propto A^{1.1}\, Re^{0.18}\, Ri^{-0.02} \qquad (7)$$

where A is the depthwise aspect-ratio of the cavity. This correlation should be quite useful for design applications, as it has a simple form and spans four decades of Ri (i.e. $0.1 < Ri < 1000$). It does not, however, provide any clues to the interaction of the two heat transfer mechanisms involved. Moreover, the experimental conditions of ref. [16] correspond to $2200 \leqslant Re \leqslant 12000$ and $10^7 \leqslant Gr \leqslant 5 \times 10^9$, which include laminar and turbulent regimes for both the forced and natural convection mechanisms. The casting of the data for the two flow regimes into one correlation had resulted in a very weak dependence of the heat transfer rate on buoyancy, which may be

justified for turbulent flows but is an anomaly for laminar flows.

It has now become a common practice in mixed convection literature [21] to correlate heat transfer results by an expression of the form

$$\overline{Nu}^n = \overline{Nu}_F^n \pm \overline{Nu}_N^n \tag{8}$$

where subscripts F and N refer to pure forced and natural convection, respectively. The value of the exponent n and the sign between the two terms on the right-hand side of the equation depend on the flow configuration and geometry. The correlations for the average Nusselt numbers $\overline{Nu}_F$ and $\overline{Nu}_N$ are determined with clues from the existing correlations for similar geometries. Equation (8) yields the correct form of dependence on the governing parameters of the problem in the two limiting cases (i.e. forced convection as $Gr \to 0$, and natural convection as $Re \to 0$), a characteristic that equation (7) does not have.

To identify a correct form for the heat transfer correlation, an expression similar to equation (8) is sought. The Nusselt number is first scaled by $Re^{0.5}$, as suggested by correlations for laminar forced convective flow over flat plates [22]. Figure 11 indicates that this scaling is appropriate as curves for different values of Re collapse on one another, for the entire range of Ri examined. The heat transfer results for $Pr = 0.01$ and $Re = 500$ do not follow a trend similar to the other curves in the figure, and will not be considered for finding the correlation. This is justified by the fact that the heat transfer for this set of conditions is mostly via conduction (i.e. $Nu = 1.03$). In finding the form of dependence of Nu_F on Pr, two ranges are considered, namely, $Pr \leqslant 1$ and $Pr \geqslant 1$. Least-squares fits of the data at $Ri = 0.01$, which may be regarded as pure forced convection, provide the following relations:

$$\overline{Nu}_F \propto \begin{cases} Pr^{0.4} & \text{for} \quad Pr < 1 \\ Pr^{0.36} & \text{for} \quad Pr > 1 \end{cases}. \tag{9}$$

These are in agreement with the results for heat transfer over a flat plate which are proportional to $Pr^{1/2}$ and $Pr^{1/3}$ for $Pr < 1$ and $Pr > 1$, respectively [22].

To find the correct form of variation of $\overline{Nu}$ with Ri and Pr for the mixed and natural convection regimes, it is first noted that Ri is not the correct scaling parameter for both $Pr > 1$ and $Pr < 1$ conditions, as the curves for $Pr \leqslant 1$ in Fig. 11 have knees at around Ri equal to unity, while other curves in the figure seem to have departures from pure forced convection mechanism at values of Ri greater than unity. This is in agreement with the scaling analysis of Bejan [18] for mixed convection heat transfer over a vertical wall, which suggests use of different scaling criteria for transition from forced convection to natural convection regimes. These criteria are

for $Pr < 1$ fluids

$$Ri^{1/4} \begin{cases} < O(1) & \text{forced convection} \\ > O(1) & \text{natural convection} \end{cases} \tag{10}$$

and for $Pr > 1$ fluids

$$\left(\frac{Ri}{Pr^{1/3}}\right)^{1/4} \begin{cases} < O(1) & \text{forced convection} \\ > O(1) & \text{natural convection} \end{cases}. \tag{11}$$

Figure 12 presents the variation of $\overline{Nu}$ scaled with $Re^{0.5} \times Pr^m$ against the scaling parameters of equations (10) and (11), depending on the range of Pr. The exponent m also depends on the range of Pr as given by equation (9). This figure indicates the proper scaling of both the abscissa and ordinate, and shows the correct forced convection and natural convection limits for both ranges of Pr. The Nu variations in the natural convection limit seem to be proportional to the abscissa parameter raised to the 0.20 power, rather than the 1/4th power suggested by criteria of equations (10) and (11). From this figure it may be concluded that the overall effect of buoyancy in the cavity is to assist the heat transfer, and no opposing effects

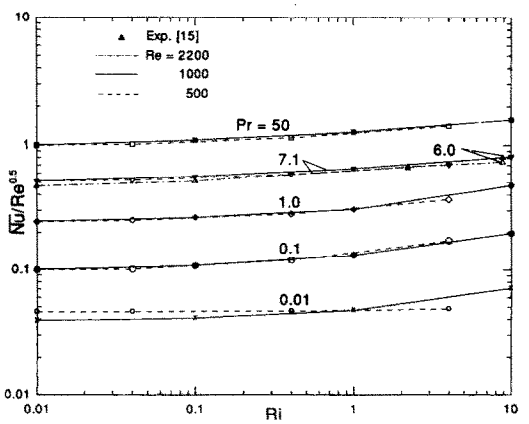

FIG. 11. Variation of averaged Nu scaled by $Re^{0.5}$ with Ri for different values of Pr.

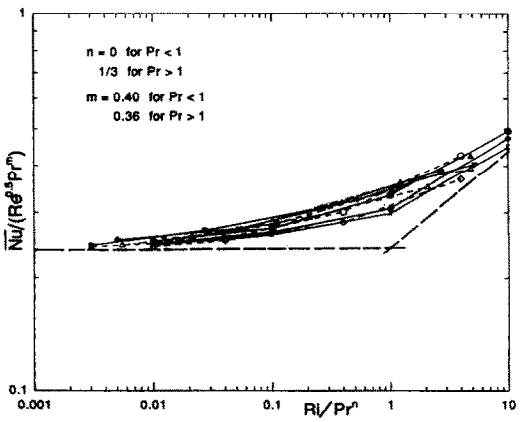

FIG. 12. Variation of heat transfer in the cavity as a function of Re, Ri, and Pr (symbols are the same as those of Fig. 11).

appears to be present for the range of parameters examined.

5. CONCLUSIONS

The flow and heat transfer is investigated in a bottom heated lid-driven square cavity flow. The effects of Prandtl number on the flow structure and heat transfer in the cavity are studied for laminar ranges of Re and Gr. The influence of buoyancy on the flow and heat transfer in the cavity is found to be more pronounced for higher values of Pr, if Re and Gr are kept constant. The natural convection effects are always assisting the forced convection heat transfer, and the extent of the contribution is a function of Pr and Ri. The average heat transfer in the cavity is correlated as

$$\overline{Nu} = A\,Re^{0.5}\,Pr^{m}\left[1.0 + B\left(\frac{Ri}{Pr^{n}}\right)^{q}\right] \qquad (12)$$

where A and B are constants, the exponents m and n depend on Pr, as given by equations (9) to (11), and q is a constant of the order of 0.20 to 0.25.

REFERENCES

1. C. K. Cha and Y. Jaluria, Recirculating mixed convection flow for energy extraction, *Int. J. Heat Mass Transfer* **27**, 1801–1810 (1984).
2. J. Imberger and P. F. Hamblin, Dynamics of lakes, reservoirs, and cooling ponds, *A. Rev. Fluid Mech.* **14**, 153–187 (1982).
3. F. J. K. Ideriah, Prediction of turbulent cavity flow driven by buoyancy and shear, *J. Mech. Engng Sci.* **22**, 287–295 (1980).
4. L. A. B. Pilkington, Review lecture: The float glass process, *Proc. R. Soc. Lond., 1A* **314**, 1–25 (1969).
5. R. K. Agarwal, A third-order-accurate upwind scheme for Navier–Stokes solutions at high Reynolds numbers, AIAA-81-0112, *Proc. 19th AIAA Aerospace Sciences Meeting*, St. Louis, MI, January (1981).
6. U. Ghia, K. N. Ghia and C. T. Shin, High-Re solutions for incompressible flow using Navier–Stokes equations and a multigrid method, *J. Comput. Phys.* **48**, 387–411 (1982).
7. R. Schreiber and H. B. Keller, Driven cavity flows by efficient numerical techniques, *J. Comput. Phys.* **49**, 310–333 (1983).
8. M. C. Thompson and J. H. Ferziger, An adaptive multigrid technique for the incompressible Navier–Stokes equations, *J. Comput. Phys.* **82**, 94–121 (1989).
9. D. L. Young, J. A. Liggett and R. H. Gallagher, Unsteady stratified circulation in a cavity, *ASCE J. The Engineering Mechanics Division* **102**(EM6), 1009–1023 (1976).
10. M. Morzynski and Cz. O. Popiel, Laminar heat transfer in a two-dimensional cavity covered by a moving wall, *Numer. Heat Transfer* **13**, 265–273 (1988).
11. J. R. Koseff, R. L. Street, P. M. Gresho, C. D. Upson, J. A. C. Humphrey and W. M. To, A three-dimensional lid-driven cavity flow: experiment and simulation, *Proc. 3rd Int. Conf. on Numerical Methods in Laminar and Turbulent Flow*, Univ. Washington, 8–11 August, pp. 564–581 (1983).
12. J. R. Koseff and R. L. Street, The lid-driven cavity flow: a synthesis of qualitative and quantitative observations, *ASME J. Fluids Engng* **106**, 390–398 (1984).
13. J. R. Koseff and R. L. Street, Circulation structure in a stratified cavity flow, *ASCE J. Hydraulic Engng* **111**, 334–354 (1985).
14. C. J. Freitas and R. L. Street, Non-linear transient phenomena in a complex recirculating flow: a numerical investigation, *Int. J. Numer. Methods Fluids* **8**, 769–802 (1988).
15. K. Torrance, R. Davis, K. Eike, P. Gill, D. Gutman, A. Hsui, S. Lyons and H. Zien, Cavity flows driven by buoyancy and shear, *J. Fluid Mech.* **51**(2), 221–231 (1972).
16. A. K. Prasad and J. R. Koseff, Combined forced and natural convection heat transfer in a deep lid-driven cavity flow, in *Heat Transfer in Convective Flows*, **HTD-107**, pp. 155–162. ASME, New York (1989).
17. J. R. Lloyd and E. M. Sparrow, Combined forced and free convection flow on vertical surfaces, *Int. J. Heat Mass Transfer* **13**, 434–438 (1970).
18. A. Bejan, *Convective Heat Transfer*, pp. 141–146. Wiley, New York (1984).
19. A. A. Mohamad and R. Viskanta, Effects of the upper lid shear on the stability of flow in a cavity heated from below, *Int. J. Heat Mass Transfer* **32**, 2155–2166 (1989).
20. S. V. Patankar, *Numerical Heat Transfer and Fluid Flow*. McGraw-Hill, New York (1980).
21. F. P. Incropera and D. P. DeWitt, *Fundamentals of Heat and Mass Transfer*, 3rd Edn. Wiley, New York (1990).
22. W. M. Kays and M. E. Crawford, *Convective Heat and Mass Transfer*, 2nd Edn. McGraw-Hill, New York (1980).

EFFET DU NOMBRE DE PRANDTL SUR LA CONVECTION THERMIQUE MIXTE LAMINAIRE CONDUITE DANS UNE CAVITE PAR SON COUVERCLE

Résumé—On considère l'écoulement et le transfert de chaleur dans une cavité carrée pour laquelle le mouvement du fluide est induit par le frottement résultant du mouvement de translation du couvercle et par la force de flottement due au chauffage du plancher. Cette étude est motivée par l'application à la production du verre plan dans laquelle celui-ci est poussé sur un bain de métal liquide, puis refroidi et solidifié. Les simulations numériques sont faites pour un écoulement laminaire bidimensionnel ($100 \leqslant Re \leqslant 2200$) et, pour différentes valeurs du nombre de Richardson, on étudie les effets du nombre de Prandtl depuis les valeurs faibles ($0{,}01 < Pr < 50$) sur l'écoulement et le transfert de chaleur dans la cavité. La température et le champ d'écoulement sont calculés et présentés pour illustrer la forte influence du nombre de Prandtl. Les nombres de Nusselt locaux et globaux sont aussi rapportés pour différentes valeurs de Re, Ri et Pr.

EINFLUSS DER PRANDTL-ZAHL AUF DEN WÄRMEÜBERGANG BEI LAMINARER MISCHKONVEKTION IN EINEM HOHLRAUM MIT BEWEGTER DECKFLÄCHE

Zusammenfassung—Die vorliegende Arbeit beschäftigt sich mit der Strömung und dem Wärmeübergang in einem quadratischen Hohlraum, wobei die Strömung durch die Reibungskraft als Folge der Bewegung der oberen Deckfläche, in Verbindung mit der Auftriebskraft als Folge der Bodenheizung verursacht wird. Die Arbeit wurde durch ihre Bedeutung für die Produktion von Flachglas angeregt. Dort werden die Glasscheiben über ein Bad mit flüssigem Metall gezogen, während sie gekühlt werden und erstarren. Aus diesem Grund werden die numerischen Simulationsrechnungen für zweidimensionale laminare Strömung ($100 \leqslant Re \leqslant 2200$) im Bereich kleiner bis mittlerer Prandtl-Zahlen durchgeführt ($0{,}01 < Pr < 50$). Der Wärmeübergang im Hohlraum wird für unterschiedliche Werte der Richardson-Zahl untersucht. Um den starken Einfluß der Prandtl-Zahl zu verdeutlichen, werden die Temperatur- und Strömungsfelder im Hohlraum dargestellt. Darüberhinaus werden lokale und mittlere Nusselt-Zahlen für verschiedene Werte von *Re*, *Ri* und *Pr* präsentiert.

ВЛИЯНИЕ ЧИСЛА ПРАНДТЛЯ НА ТЕПЛОПЕРЕНОС ПРИ ЛАМИНАРНОЙ СМЕШАННОЙ КОНВЕКЦИИ В ПОЛОСТИ С ДВИЖУЩЕЙСЯ КРЫШКОЙ

Аннотация—Исследуются течение и теплоперенос в квадратной полости, в которой течение вызвано сдвиговой силой, обусловленной движением верхней крышки, и подъемной силой за счет нагрева основания. Исследование выполняется с целью использования его результатов при производстве плоского стекла, в процессе которого охлаждаемый и затвердевающий стеклянный лист вытягивается из ванны с расплавленным металлом. В связи с этим проводится численное моделирование для двумерного ламинарного течения ($100 \leqslant Re \leqslant 2200$) и исследуется влияние числа Прандтля от малых до умеренных значений (т.е. $0{,}01 < Pr < 50$) на течение и теплоперенос в полости при различных значениях числа Ричардсона. Сильное влияние числа Прандтля иллюстрируется численными результатами для полей температур и течения в полости. Представлены также локальное и среднее числа Нуссельта при различных значениях *Re*, *Ri* и *Pr*.